Journal of Power Sources 190 (2009) 461–475

Contents lists available at ScienceDirect

Journal of Power Sources

journal homepage: www.elsevier.com/locate/jpowsour

Thermodynamic evaluation of small-scale systems with biomass gasifiers, solid oxide fuel cells with Ni/GDC anodes and gas turbines

P.V. Aravind*, T. Woudstra, N. Woudstra, H. Spliethoff[1]

Section Energy Technology, Department of Process and Energy, TU Delft, Leeghwaterstraat 44, 2628 CA Delft, The Netherlands

ARTICLE INFO

Article history:
Received 13 October 2008
Received in revised form 7 January 2009
Accepted 10 January 2009
Available online 20 January 2009

Keywords:
Biomass gasifier
Solid oxide fuel cell
Exergy

ABSTRACT

Thermodynamic calculations were carried out to evaluate the performance of small-scale gasifier–SOFC–GT systems of the order of 100 kW. Solid Oxide Fuel Cells (SOFCs) with Nickel/Gadolinia Doped Ceria (Ni/GDC) anodes were considered. High system electrical efficiencies above 50% are achievable with these systems. The results obtained indicate that when gas cleaning is carried out at temperatures lower than gasification temperature, additional steam may have to be added to biosyngas in order to avoid carbon deposition. To analyze the influence of gas cleaning at lower temperatures and steam addition on system efficiency, additional system calculations were carried out. It is observed that steam addition does not have significant impact on system electrical efficiency. However, generation of additional steam using heat from gas turbine outlet decreases the thermal energy and exergy available at the system outlet thereby decreasing total system efficiency. With the gas cleaning at atmospheric temperature, there is a decrease in the electrical efficiency of the order of 4–5% when compared to the efficiency of the systems working with intermediate to high gas-cleaning temperatures.

1. Introduction

Solid Oxide Fuel Cells (SOFCs) are devices, which produce electricity and heat using fuels such as hydrogen, carbon monoxide, methane or using a mixture of them. When operated at high pressures, they can be combined with gas turbines for obtaining very high efficiency for electricity generation. Use of biosyngas from biomass gasifiers as fuel for such systems is a topic, which is attracting significant attention from scientific community [1–9]. Such systems offer an opportunity for realizing sustainable, highly efficient and practically carbon neutral electricity generation.

Preliminary system studies carried out before with biomass gasifier–SOFC–gas turbine systems have indicated high electrical efficiencies of around 50% for gasifier–SOFC–gas turbine systems of few hundred kW power level [9]. In gasifier–SOFC–GT systems, it is possible to employ low-temperature or high-temperature gas-cleaning options. Low-temperature gas-cleaning systems are said to be more reliable and can probably achieve high levels of gas cleaning required effectively. On the other hand, it is widely suggested that high-temperature gas-cleaning systems may bring significantly higher efficiencies and reduce the need of heat transfer in these systems. However, high-temperature gas-cleaning systems are still in developing stage. For a variety of contaminants like particulates, tar, alkali compounds and acid gases, different cleaning systems working at different temperature levels are widely suggested in literature [1]. To have all these different cleaning systems at or near the gasifier outlet temperatures, which are usually in the range of 973–1173 K is a challenging task.

This paper presents the results from thermodynamic analysis of systems with biomass gasifiers, solid oxide fuel cells and gas turbines of power levels near 100 kW. SOFCs with Nickel/Gadolinia Doped Ceria (Ni/GDC) anodes are considered for the present study as they are expected to have advantages for biosyngas based systems due to better contaminant tolerance [1,3]. The knowledge generated from experimental studies about the influence of biomass derived contaminants on performance of SOFCs with Ni/GDC anodes as well as the information available on gas-cleaning technologies is used to arrive at concepts for high-temperature gas-cleaning methods for gasifier–SOFC–gas turbine systems [1,3,10]. This paper presents a set of options for gas-cleaning systems. However, it is not intended to provide details of the designs for various cleaning systems as these systems are still under various stages of research and development. Instead, possible gas-cleaning processes and their proposed operation parameters are briefly mentioned. Selection of the cleaning method for gasifier–SOFC–gas turbine systems will finally depend upon the trade offs between system feasibility, cost and thermodynamic consequences of employing the particular choice. Thermodynamic analysis presented here is expected to add further clarity in such discussions.

* Corresponding author.
E-mail address: p.v.aravind@tudelft.nl (P.V. Aravind).
[1] Presently at Institute of Energy Systems, TU Munich, Boltzmannstrasse 15, 85748 Garching, Germany.

0378-7753/$ – see front matter © 2009 Elsevier B.V. All rights reserved.
doi:10.1016/j.jpowsour.2009.01.017

Since carbon deposition is a problem expected when temperature of biosyngas is varied [1], thermodynamics of carbon deposition and the influence of steam addition to the fuel gas on carbon deposition are discussed. Requirement of steam addition to suppress carbon deposition thermodynamically at different temperatures of gas cleaning is calculated. A base case system is presented with lowest gas-cleaning temperature at 873 K. Since fuel cell systems and gas turbine cycles are sensitive to steam addition, thermodynamic system calculations with different temperature levels for gas cleaning and hence with different levels of steam addition, yielding possible efficiencies that can be achieved with such systems are also presented.

2. Description of subsystems employed

The proposed systems consist of a biomass gasifier, a gas-cleaning system, a solid oxide fuel cell and a gas turbine as shown in Fig. 1. The biosyngas from the gasifier is cleaned and is fed to

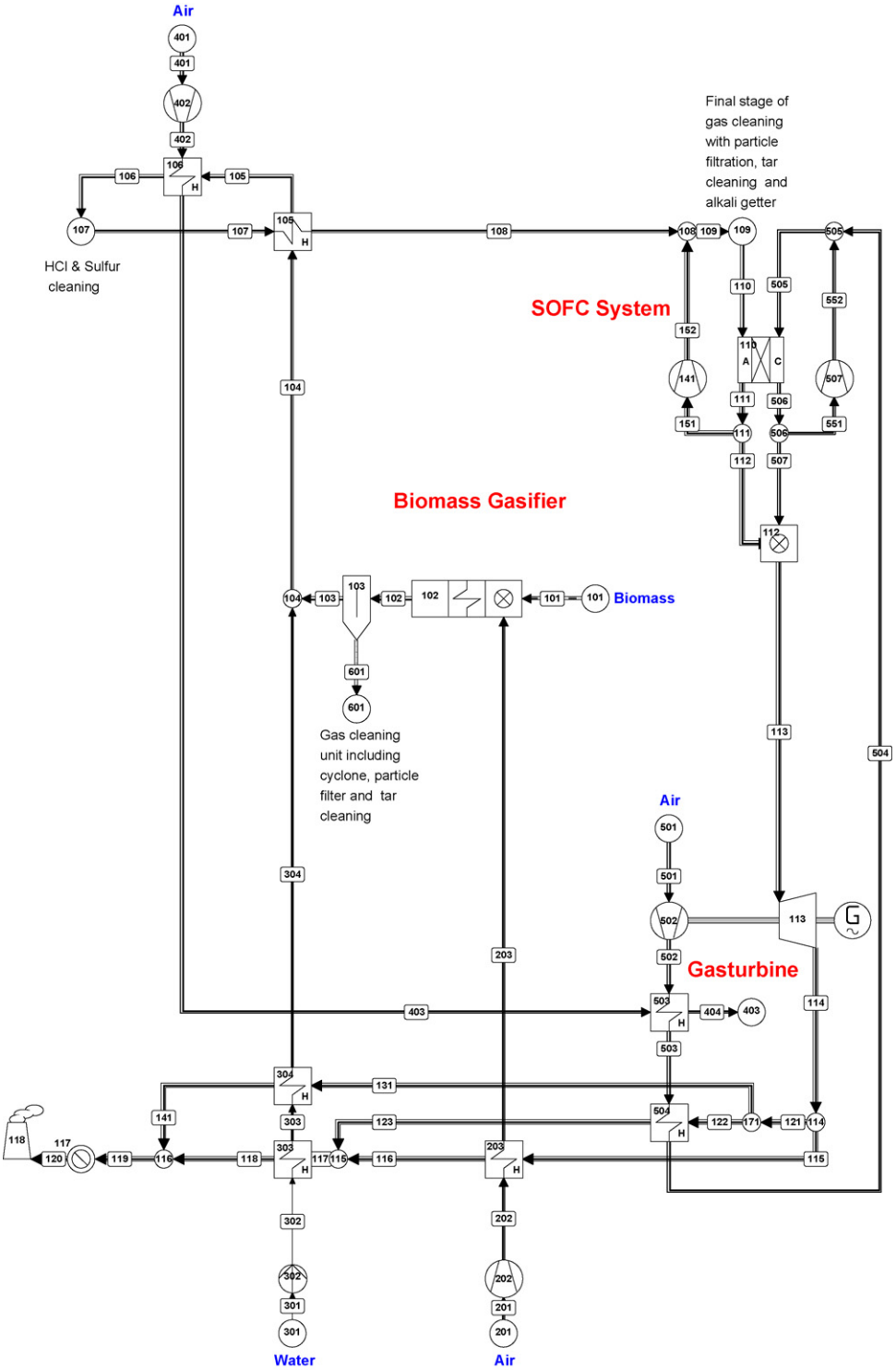

Fig. 1. Flow diagram for the base case system.

Table 1
Biosyngas composition from IISc gasifier and biosyngas composition from the gasifier model employed at atmospheric pressure.

No.		Gas composition (vol.%)					
		H_2	CO	CO_2	H_2O	CH_4	N_2
1	Biosyngas from IISc gasifier with clean wood as fuel	18–20	17–19.5	12–14	3	1.5	40–45
2	Biosyngas from the gasifier model (without adjusting moisture%)	18.4	18.4	11.3	10.4	1.46	39.6
3	Biosyngas from the gasifier model (after adjusting moisture%)	19.8	19.8	12.2	3	1.58	42.7

the fuel cell. Unspent air from the cathode outlet stream is used to combust the unspent fuel. The flue gas is fed to the turbine. Turbine exhaust is used to preheat the cathode inlet air, air for gasification, and for generating the steam required. These systems have following subsystems.

2.1. Gasifier subsystem

Gasifiers considered here are fixed bed gasifiers working at high pressures. Air gasification is selected for the present study for the following reasons, i.e., (1) fixed bed co-current air gasification offers comparatively low tar in the gas generated, (2) though nitrogen in air used for gasification may cause exergy destruction in the gasifier, it may reduce the requirement of extra cooling air at the cathode of the SOFC and hence may reduce exergy loss in the SOFC there by compensating (at least partly) the loss in the gasifier and (3) air gasification generates less methane in the gas compared to steam gasification (contaminants such as H_2S or tar in the gas will affect the methane reforming inside the SOFC as reported in literature) [1,5]. Fixed bed downdraft air gasification systems appear to produce biosyngas compositions which are close to equilibrium compositions. To verify this assumption, the gasification process in such gasifiers is modeled using Cycle-Tempo [11]. A comparison is made between the calculated values of the gas compositions and the experimentally recorded values from the fixed bed open top co-current downdraft gasifier with twin air entry designed by Indian Institute of Science (IISc). These gasifiers work at atmospheric pressures and hence the comparison between calculated values and measured values were carried out only at atmospheric pressures. Details of these gasification systems are available elsewhere [12]. A high-pressure fixed bed gasifier based on the same process concept is also being developed but no additional information is available about this high-pressure gasification system. Reported gas composition from these gasifiers, measured experimentally (working at atmospheric pressure), with clean wood as fuel is given in Table 1. All the values are given in volume percentage.

For the equilibrium calculations, a gasifier gas outlet temperature of 1073 K is assumed. A part of the carbon is removed from the gasifier system representing the losses usually occurring in gasifiers (Usually in fixed bed downdraft gasifiers, this is the part of solid carbon in biomass which do not get converted in the gasification reaction and get removed from the bottom of the reactor often together with ash). Here it is assumed that 5% of the carbon remains unconverted and is removed.

It is reported that casaurina with 10–12% moisture is used for the experiments reported with IISc gasifier and the exact composition of the biomass was not given. For that reason, composition of casaurina was taken from Phyllis database for biomass (provided by Energy research Center of the Netherlands) [13]. The following composition is used. C 49.3%, H 5.9%, N 0.6%, O 44%, S 0.02% and Cl 0.162%. (It is assumed that the biomass contains 12% moisture. As the dry composition is given, it is changed by adding 12% moisture for the calculations). Methane formation is not shown in the equilibrium calculations since when equilibrium is attained, methane is not expected to be present in the gas. Usually, the biosyngas does not attain complete equilibrium composition in the gasifiers (as indicated by the presence of methane). For this reason, gas composition had to be manipulated to get the calculated composition comparable to the observed composition. For this, the biomass composition is readjusted by adding 4% by mass methane while keeping the C:H:O ratio in the biomass same. A part of this methane is then bypassed in the gasification reactor so that the outlet gas has around 1.5% methane by volume. Similarly, the calculations give composition at the assumed gasifier exit temperature of 1073 K where as the literature indicate the quench gas composition at room temperature and for this reason the moisture content in the gas is reduced to 3% (as it is reported in literature) and the gas composition is then readjusted. The gas compositions obtained from the equilibrium calculation after the corrections for methane with and without adjusting for moisture fraction are given in Table 1. It can be seen that the gas composition from the model calculation after adjusting for moisture is in reasonable agreement with the reported composition from the IISc gasifier. It is observed that the calculated percentage value of carbon monoxide is slightly more than the measured value. This variation in the calculated and observed gas compositions is considered as not significant enough to produce differences in the trends observed in the system performance from this work. For the system calculations, the lower heating value of biomass is given as a constant value independent of the biomass composition. Modeling approach used for accounting for the methane presence in the syngas generated is not expected to affect the system efficiencies calculated significantly. For these reasons, the gasification model from Cycle-Tempo, in its modified form, is accepted for detailed system calculations. No comparison is carried out with measured and calculated values of compositions for higher pressures, as there is no measurement data available. However, it is assumed that it is possible to design such gasifiers giving biosyngas at equilibrium conditions while working at higher pressure values.

2.2. Gas-cleaning subsystem

It is desirable to have the gas-cleaning temperature in between the gasifier outlet temperature and the SOFC inlet temperature. However, there are limitations with known viable gas-cleaning options to reach the gas-cleaning requirements of SOFCs operating at these temperatures as reported elsewhere [1]. The base case system is presented with a high-temperature gas-cleaning concept, expected to work at or above 873 K, which is lower than the gasification temperature and the SOFC inlet temperature. Proposal for this gas-cleaning system is based on detailed literature study, chemical equilibrium analysis and preliminary experiments[1,3,10]. It is assumed that all the contaminants are required to be cleaned to few ppm levels. Results from the base case system are later compared with results from systems with different lowest cleaning temperatures.

Possibility of SOFCs working with rather high level of contaminants in biosyngas (though required to be confirmed with extensive studies) brings in the opportunity to consider gas-cleaning systems working at very high temperatures close to that of gasification (usually resulting in less effective gas cleaning). For this reason,

an additional gas-cleaning concept is presented in Appendix A in which the gas cleaning takes place at the gasifier exit temperature.

2.2.1. Carbon deposition in gasifier–fuel cell systems and ternary diagrams

Heating or cooling of biosyngas will influence its composition. One consequence of varying the temperature is the precipitation of solid carbon in the gas-heating element or gas-cooling element. Thermodynamic equilibrium composition may or may not be achieved at various temperatures depending upon how fast the reactions involved are at the given temperature. However, the equilibrium analysis tells us about the thermodynamic constraints existing for reactions causing carbon deposition at given conditions. Carbon deposition can cause blocking of the gas pipes and this may result in detrimental consequences in the system operation.

Carbon deposition depends on C–H–O equilibrium at given temperature and pressure. Higher concentrations of oxygen and hydrogen in the fuel reduce the carbon deposition tendencies. SOFC operation with biosyngas as a fuel is reported in literature. Carbon deposition from synthetic biosyngas is observed during the heating of the gas in the fuel pipe on its way to the fuel cell anode. However, it was possible to suppress carbon deposition by addition of steam [1]. There was no carbon deposition on the cell anode surface. This is expected as the higher temperature at the anode and higher oxygen fraction when the cell is generating current are expected to suppress the deposition tendency at the anode. This in turn implies that the passage of the gas from the gasifiers through the gas-cleaning and conditioning systems to the fuel cell inlet has to be controlled carefully to avoid carbon deposition. In the work presented in this paper, carbon deposition tendencies of various gas compositions are analyzed using Factsage, a software for chemical equilibrium calculations [14].

For a given gas composition (Composition number 2 from Table 1) representing the outlet gas composition from a fixed bed downdraft air fed gasifier at 1 bar and at 1073 K, Fig. 2a gives the variation in carbon deposition tendencies with varying temperature and shows the presence of solid carbon if the gas is cooled. The ternary (Fig. 2b) diagram shows the carbon deposition tendencies. Solid lines inside the triangle indicate carbon boundary lines. Above the carbon boundary line, solid carbon exists in heterogeneous equilibrium with the gas phase components. Below the carbon boundary line no solid carbon is present. Once the composition of a fuel gas is known, its coordinates in the ternary diagrams can be identified. If the fuel gas temperature is known, carbon boundary line can be drawn.

The point representing the given biosyngas composition above is safe with respect to the carbon deposition at 1173 K and at 973 K as it is shown in the ternary diagram. If the gas is cooled now to 773 K, it can be seen that the point is above the carbon boundary line and is in the carbon deposition region. If a given gas composition is in carbon deposition region, addition of steam will increase the fraction of hydrogen and oxygen atoms and will bring the coordinates representing fuel composition further down towards the carbon boundary line. When sufficient steam is added, the coordinates representing the gas composition will be in carbon free region. For the case presented here, the point with steam added in the diagram indicates the composition of the gas given above with 30% steam (of the initial gas flow, given as vol.%). It can be seen that the gas is now safe with respect to carbon deposition even at 773 K. For the same fuel gas, once it enters the SOFC anode, since the oxygen fraction in the gas increases as the gas passes through the anode chamber (when the fuel cell is producing current), the gas composition moves further away from the carbon deposition region. Similar is the effect of temperature. As the temperature increases, the deposition region shrinks towards higher carbon concentration

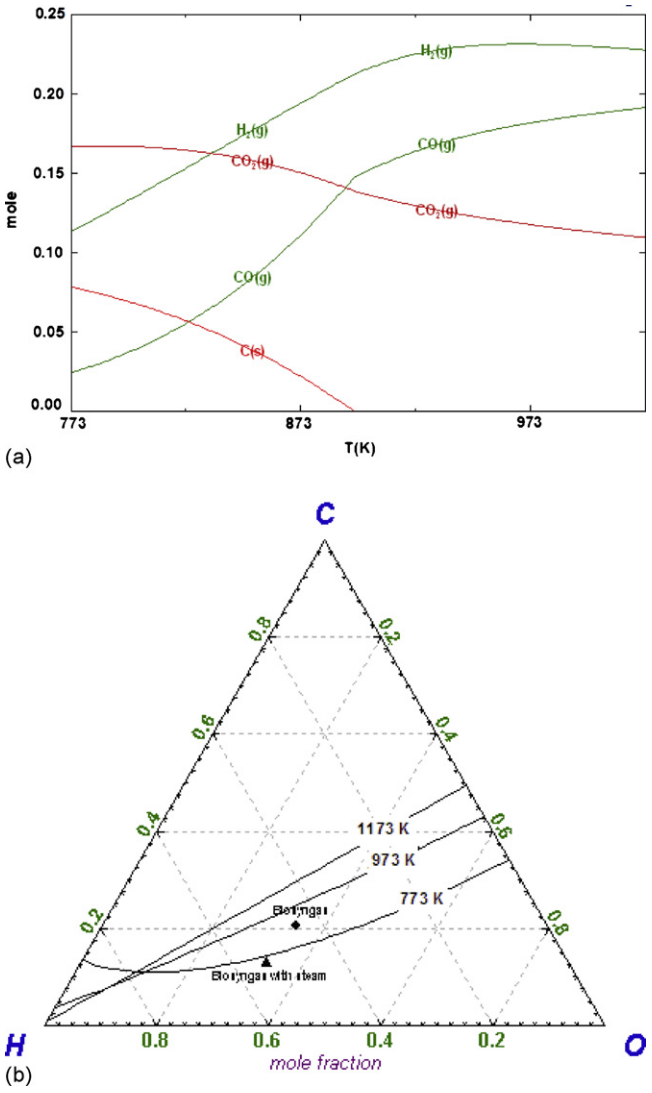

Fig. 2. (a) Carbon deposition behavior with biosyngas. (b) Ternary diagram indicating carbon deposition region.

region within the temperature range considered in this work (up to 1273 K).

2.3. The fuel cell system

SOFCs considered here are the ones based on Ni/GDC anodes and Lanthanum Strontium Manganite (LSM) cathodes working at temperatures above 1123 K. As the SOFCs are still in a developing stage, no relevant data about the stack performance using biosyngas are available. However, the cell performance using various biosyngas compositions is reported before [1,5]. Based on these results, reasonable assumptions are taken for the values for different parameters such as cell resistance and current density for the calculations presented in this paper.

2.4. The gas turbine and heat recovery

The gas turbine considered in this system is of 30 kW power level. Mass flows through the system and hence the power level is set by the turbine power fixed at 30 kW. It is not considered that the system represents any of the available commercial gas turbines. However, we assume that it is possible to design turbines with the specific characteristics mentioned in this study. Values for

isentropic efficiencies and mechanical efficiencies for the turbine and the compressor are taken based on literature available for a similar capacity Capstone turbine. In the present system model, cathode and anode outlet gases are partly recirculated as shown in Fig. 1. Rest of the anode and cathode gases are fed to the combustor and the combusted mixture is fed to the gas turbine inlet. Turbine outlet gas is used for preheating the cathode air, gasification air and for generating the additional steam needed. A sink representing a heat consumer is included in the process scheme before the stack to recover the thermal energy at the exit of which the gas temperature is reduced to 373 K before it is fed to the stack. It is assumed that this energy can be used for other external applications such as space heating, water heating or small-scale food processing industries.

Preheating of the gasification air using the turbine exhaust split stream is suggested for the models considered in this paper since this is expected to increase the system efficiency. However, since the preheating is expected to change the oxygen required for gasification, and hence the gas composition, steam required to be added to prevent carbon deposition may vary. This will cause variations in system performance by influencing the performance of system components such as the SOFC and the gas turbine. For this reason, a comparison is also made between such systems with and without preheating the gasification air. Results from these calculations are given in Appendix B.

2.5. SOFC gas turbine combination

The cooling air required to keep the fuel cell at the required operating temperature varies with the fuels used. Possibility of including endothermic reforming reactions in the anode chamber helps to increase the fuel cell efficiency. When methane is there in the fuel, its reforming is endothermic. Reduced cathodic airflows also shall alter the SOFC–GT system efficiencies with reduced requirement of compression work and heating for cathodic air supply thereby increasing the system efficiency. For SOFC–GT systems, efficiency values around 70–80% had been reported in the literature with natural gas as fuel. The basic SOFC–GT combination presented in this work fed with methane is modeled and the efficiency obtained with steam–methane mixture is around 78% [1]. This value compares well with the other system configurations presented in literature [15].

3. Component models and system efficiencies

Thermodynamic calculations are carried out using Cycle-Tempo, an in-house software developed at section energy technology, TU Delft. Cycle-Tempo employs a Gibbs free energy minimization based routine for equilibrium calculations in the gasifier model, combustor model and in the fuel cell model used in these calculations. Details of these models are available in the Cycle-Tempo manual. For the gasifier, the Cycle-Tempo model is considered based on the discussions presented in the part of this paper where different subsystems are described.

In the present work, the power level given for the turbine and other related parameters determine the mass flow through the turbine and hence through the system. The energy balance at the fuel cell determines the cathode airflow based on the cooling air required. These two subsystems, namely the fuel cell subsystem and the gas turbine subsystem together play an important role in determining the inlet biomass flow. For these reasons, variations in the system performance can be better understood with the basic equations governing the processes in the fuel cell and the gas turbine as used in the Cycle-Tempo calculations [11]. These equations are given below.

For the fuel cell, the model first takes the inlet gas to the equilibrium conditions. Then, the active cell area, the cell voltage V, the current flow I and the electrical output power P_e are calculated. It is supposed that the processes occur at a constant temperature and pressure. The flow through the fuel cell anode, $\Phi_{m,a,in}$ related to the total current as given in the following equation:

$$I = \frac{\Phi_{m,a,in}}{M_a} 2F(y^0_{H_2} + y^0_{CO} + 4y^0_{CH_4})U_F \quad (1)$$

Here, y^0_i are the concentrations at the inlet, M_a is the mole mass of the anode gas, F is the Faraday constant and U_F is the fuel utilization. The mass flow of the oxygen from cathode to anode is calculated based on the current flow. Energy balance determines cathode airflow since the temperature at the outlet is given. To calculate current density i_m, voltage V and electrical power P_e, a one-dimensional model of the active cell area is used. That is, the temperatures, pressures and compositions are supposed to be constant in a cross-section, perpendicular to the direction of the fuel cell flow. The following local variables (indicated with the index x) are calculated:

- Reversible voltage $V_{rev,x}$
- Current density i_x
- Concentrations y_x (H_2, CO, H_2O, CO_2 and CH_4)

If the processes in a cross-section x of the fuel cell occur without losses, the cell voltage is identical to the reversible voltage or Nernst voltage. For the SOFC, the reversible voltage, if the gases are supposed to behave ideally, is given as

$$V_{rev,x} = V^0_{rev} + \frac{RT}{2F} \ln\left\{ \frac{y^{1/2}_{O_2,c} y_{H_2,a}}{y_{H_2O,a}} \times P^{1/2}_{cell} \right\} \quad (2)$$

where V^0_{rev} is the standard reversible voltage for hydrogen, R is the universal gas constant, T the temperature, y the mole fraction at the cross-section, and P is the pressure. In the model, it is assumed that the voltage losses on the level of the electrodes are negligible in the x-direction. This means that the cell voltage is supposed to be constant over the fuel cell. Thus

$$\Delta V_x = V_{rev,x} - V \quad (3)$$

where ΔV_x is the voltage loss. Then the current density in the cross-section x is

$$i_x = \frac{\Delta V_x}{R_{eq}} \quad (4)$$

where R_{eq} is the equivalent cell resistance.

Over the whole cell, these quantities are connected with the following equation:

$$\frac{I}{A} = \frac{U_F}{R_{eq} \int_0^{U_F} d\lambda/(V_{rev} - V)} \quad (5)$$

where I is the total current, A is the cell area and λ is the dimensionless reaction coordinate. Once the current and the voltage are known, the power can be calculated.

For the turbine, the outlet enthalpy of the expanded gas is calculated as

$$h_o = h_i - \eta_s(h_i - h_{o,s}) \quad (6)$$

And for a compressor it is calculated as

$$h_o = h_i + \frac{(h_{o,s} - h_i)}{\eta_s} \quad (7)$$

where h_o is the outlet specific enthalpy, h_i is the inlet specific enthalpy, η_s is the isentropic efficiency and h_s is the specific enthalpy when the gas is isentropically expanded. Once the change

in the enthalpy is known, the mass flow required can be computed if the power level of the turbine is known.

3.1. Energy and exergy calculations

Energy efficiency calculations provided in the tables are based on the Lower Heating Value of the fuel. Electrical efficiency as well as the total efficiency including the heat available at the system outlets is provided as the results.

Cycle-Tempo can perform exergy calculations, the results of which form the basis for an exergy analysis of the system under consideration. Definition of the exergy efficiency often varies and accepting a clear definition is important for exergy efficiency calculations.

Exergy efficiency can be defined as

$$\eta_{Ex} = \frac{\sum Ex_{products}}{\sum Ex_{source}} \quad (8)$$

where $\Sigma Ex_{product}$ is the exergy of that part of the outgoing process and energy flows that can be considered to be a product of the system and ΣEx_{source} is the exergy of that part of the ingoing process and energy flows that can be considered necessary for making the product in the present process. Further specification of $Ex_{product}$ and Ex_{source} is needed to enable the calculation of the efficiency value. This will depend on the process considered and objectives of the evaluation.

For a power plant, plant electrical exergy efficiency and total system exergy efficiency are important.

The system electrical exergy efficiency is given as

$$\eta_{ex,el} = \frac{\sum P_{el,out} - \sum P_{el,in}}{Ex_{fuel,in}} \quad (9)$$

And the total exergy efficiency is calculated as

$$\eta_{ex,tot} = \frac{\sum P_{el,out} + \sum Ex_{heat,out} - \sum P_{el,in}}{Ex_{fuel,in}} \quad (10)$$

Details of definitions for various efficiency values are available with the website for Cycle-Tempo [11].

4. Process calculations with the base case system

4.1. Initial assumptions and input parameters

A flow diagram for the base case system is given in Fig. 1. Following are the major assumptions taken and the input parameters assigned. The gasification subsystem is modeled with the modifications as discussed in Section 2.1. The solid carbon remaining is separated out in the separator. Tar formation is ignored in the thermodynamic calculations. Biomass (with clean wood) composition used for the gasifier feed (dry composition) in the model calculations is given in Table 2. Carbon loss from gasifier and the methane presence is incorporated in the calculations in the same way they were included in Section 2.1.

Table 2
Biomass composition used.

Component	%Weight
C	49.9
H	6.1
N	0.47
O	42.5
S	0.035
SiO_2	0.8

4.2. The base case system and gas cleaning

It is suggested that a part of the gas cleaning can be done at a temperature, near the exit temperature of the gasifier, which is 1073 K. The suggested gas-cleaning system includes a high-temperature ceramic particulate filter working at 1073 K. A dolomite based tar-cleaning reactor is then followed. Apparatus no. 103 in Fig. 1 represents both particulate and tar-cleaning devices. Optionally, an alkali getter can also be suggested at this point. Once the cleaning for particulate and tar are over, the gas temperature is reduced for HCl and H_2S cleaning. Biosyngas is cooled from 1073 K to 873 K using a set of two heat exchangers. Steam is added before the gas temperature is brought down since the preheated steam helps to avoid carbon deposition at low-temperature regions the gas pass through, before it enters the fuel cell. Steam added is given as 14.44% of the biosyngas flow (by mass%) after the tar cleaning. The gas is then cooled to 873 K for HCl and H_2S cleaning. HCl cleaning is done using a sodium carbonate-based reactor and H_2S cleaning is carried out using a zinc titanate-based reactor. Apparatus no. 107 in Fig. 1 represents both HCl and H_2S cleaning devices. In the base case system presented here, the first heat exchanger reduces the temperature to 1004 K and an additional supply of air is used in the second heat exchanger to bring down the temperature to 873 K. Hot air from this heat exchanger is employed for heating the compressed air for the cathode. After the HCl and H_2S cleaning, the gas is heated using the first heat exchanger to 1030 K and then is mixed with a fraction of the anode outlet to increase the gas temperature to 1173 K, which is the fuel cell inlet temperature. At this point a nickel-based tar cracker is used to catalytically crack the higher hydrocarbons in the gas. An additional alkali getter is employed to bring down alkalis reemitted from the HCl cleaning section. Apparatus no. 109 in Fig. 1 represents final particulate, tar and alkali cleaning devices. It is assumed that gas-cleaning devices cause pressure drops in the system. The pressure drop in the cleaning devices combined together amounts to 0.14 bar. It is assumed that the heat lost to the environment is negligible from the whole system.

In the system presented here, cleaned gas is fed to the SOFC. As a few ppms of H_2S is expected in the fuel gas, an additional internal sulfur tolerant methane reformer with direct heat exchange with the stack, operating at stack temperature is proposed. At the anode outlet, which is at 1273 K, a fraction of the gas is recirculated and the rest is fed to the combustor. Once mixed with the recirculated anode exit gas, the fuel gas temperature is increased to 1173 K. The cathode air is compressed first and then is heated with the waste heat from the fuel gas-cleaning system. This air stream is then heated using gas turbine outlet and is fed to the cathode after adding a fraction of the cathode outlet gas, which is at 1273 K. Air is entering the cathode at 1173 K. Mass flows through the system and hence the power level is set by the turbine power fixed at 30 kW.

Turbine outlet gas is used for preheating the cathode air, gasification air and the additional steam added. The sink representing a heat consumer is included in the process scheme before the stack to recover the thermal energy at the exit of which the gas temperature is reduced to 373 K before it is fed to the stack.

In the high-temperature heat exchangers, minimum high terminal temperature difference and minimum low terminal temperature difference are taken as 30 K. A pressure drop of 0.025 bar is assumed for both primary and secondary flows.

For a commercial Capstone gas turbine system of 30 kW power level, system calculations with a hydrocarbon fuel is reported in literature[16]. It has been shown that, calculations with isentropic efficiencies of 78% and mechanical efficiencies of 98% for the turbine and the compressor shall result in the system efficiency of around 30%. This agrees well with the efficiency of 30% suggested by the manufacturer. Hence those values of isentropic and mechanical efficiencies are used in the present calculations as well. Values

Table 3
Different input parameters for various system components used for the calculations.

Isentropic efficiency for gas turbine (113)	78%
Isentropic efficiency for gas turbine compressor (602)	78%
Mechanical efficiency for gas turbine (113)	98%
Mechanical efficiency for gas turbine compressor (602)	98%
Isentropic efficiencies for other compressors, blowers and pumps	75%
Mechanical efficiencies for other compressors, blowers and pumps	95%
Generator	90%
dc/ac conversion efficiency	97%
Cell resistance	5×10^{-5} ohm m^2
Current density	2500 A m^{-2}
Fuel utilization	85%

for important parameters used in the system calculations are given in Table 3.

Detailed measurements on Ni/GDC anodes with various gas compositions including biosyngas compositions are described elsewhere [1,5]. Reasonable values for various SOFC model input parameters are assumed for present calculations based on these results. Cell resistance reported is 6×10^{-5} ohm m^2 at 1123 K and 3×10^{-5} ohm m^2 at 1193 K. For the present calculations, as a reasonable assumption, cell resistance is taken as 5×10^{-5} ohm m^2 at an average SOFC temperature of 1223 K. The mean current density is taken as 2500 A m^{-2}. Fuel utilization is taken as 85%. (85% of the incoming fuel before mixing with the recirculated anode outlet gas) and cell temperature and pressure values are taken as the mean of inlet and outlet values. The pressure drop across the fuel cell is taken as 0.05 bar. For the combustor, the pressure drop is 0.02 bar. The cell area is not given but is calculated by the program.

4.3. Results and discussion

To find the optimum pressure ratio for the gas turbine, calculations are carried out at different pressure ratios. SOFC performance is expected to improve with increase in pressure as the Nernst voltage increases with pressure as shown by Eq. (2). However, recuperated gas turbines tend to have higher efficiencies at lower pressure ratios [17]. Variation in efficiency is not very significant between pressure ratios 4.5 and 7 with highest efficiencies obtained are around 54% (Fig. 3). The system calculations presented in this work are presented at a pressure ratio of 6 for the gas turbine cycle. The pressure ratios given are taken as the ratios between the outlet pressures and the inlet pressures (absolute pressure values) of the air compressor of the gas turbine system (Apparatus no. 502 in Fig. 1)

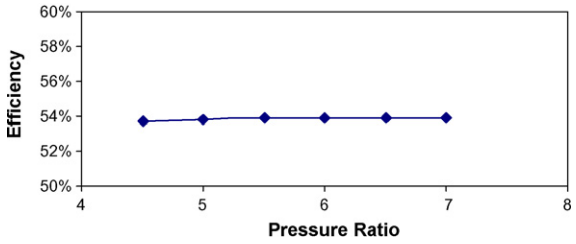

Fig. 3. Variation of electrical efficiency with pressure ratio.

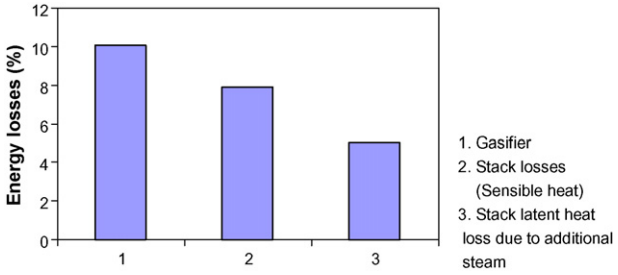

Fig. 4. Major energy losses in the system.

Table 4 summarizes the system efficiency values for the above-mentioned base case system with a pressure ratio of 6. Net electrical efficiency achieved in the system is 53.9% and the net total efficiency achieved is 72.3%. Delivered gross power is 93 kW. Delivered net power after adjusting for auxiliary power consumption is 88.5 kW. (Input energy values are given as Lower Heating Value (LHV)).

Major energy losses in the system are shown in Fig. 4. Losses during gasification, mainly because of unutilized carbon during gasification process are causing the highest energy loss followed by stack sensible heat losses (losses to the environment). Addition of steam, necessary to avoid the deposition of solid carbon in the system, increases the stack loss. This lost energy is shown as the latent heat losses through the stack. Loss in the generator is around 3.333 kW and stays same with all system calculations presented as the turbine output power is fixed. A fraction of the auxiliary power consumption for compressors and the pump is also lost (mechanical losses) and these values are significantly lower when compared to other losses and are not shown in the figure. There are also losses due to ac/dc conversion.

Fig. 5 gives an overview of the exergy losses in the system. Losses in the following subsystems are shown, i.e., (1) gasification, (2) gas-cleaning loop, (3) SOFC, (4) gas turbine, compressors, and the pump, (5) heat recovery, and (6) stack. Apparatuses included

Table 4
System efficiency with base case system.

	Apparatus	Energy flow [kW]	Totals [kW]	Exergy flow [kW]	Totals [kW]
Absorbed power	Sink/source	164.02	164.02	185.61	185.61
Delivered gross power	Generator	30.00	92.96	30.00	92.96
	Fuel cell	62.96		62.96	
Auxiliary power consumption			4.49		4.49
Delivered net power			88.47		88.47
Delivered heat	Heat sink		30.12		11.39
Total delivered			118.59		99.86
Efficiencies					
Gross		56.67%		50.08%	
Net		53.94%		47.66%	
Heat		18.36%		6.14%	
Total		72.30%		53.80%	

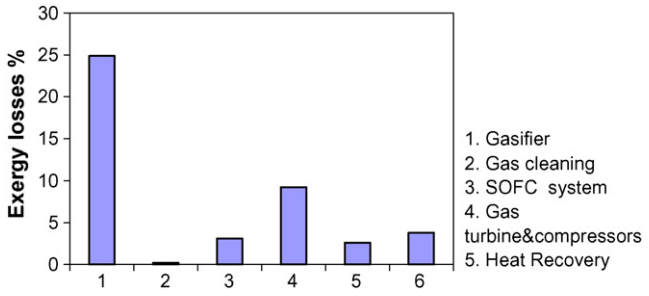

Fig. 5. Exergy losses in the system.

Table 5
Different subsystems considered.

Subsystem	Apparatuses included
Gasifier	102, 103
Gas-cleaning loop	105, 106, 107, 402
SOFC subsystem	108, 109, 110, 111, 141, 505, 506, 507
Gas turbine, compressors and the pump	502, 113, 202, 302, 112
Heat recovery	203, 303, 304, 503, 504
Stack	118

in each subsystem are given in Table 5 (apparatus numbers from Fig. 1 are given).

Gasification is a process with significant exergy destruction as hot gaseous fuel is generated from cold solid fuel and a part of the solid carbon remains unconverted. Exergy losses in gasification process are discussed in detail in literature [18]. In this work, exergy loss in gasifier is defined as the difference in total exergy value of the fuel gas and the exergy of the supplied biomass and air. The total exergy value of the fuel gas is the exergy of the gas after separation of solid carbon from the gas and preliminary gas cleaning at the gasifier outlet temperature. It can be noted that the solid carbon separated can be used in certain circumstances (for example, for activated carbon generation) and in such cases, the exergy associated with the carbon is not required to be considered as lost. This paper presents the results mainly with the assumption that the separated carbon is lost. A simplified Grassmann diagram was prepared to indicate the exergy flows within base case system. The diagram produced is given in Fig. 6.

For the gas-cleaning loop, the exergy loss is defined as the sum of the exergy losses for the fuel gas stream and the cooling fluid employed. For the cooling fluid, the exergy carried by the fluid as well as the power input for the compressor are considered as exergy input. For the fuel cell part, the exergy loss is taken as the sum of the losses for the fuel cell and the gas recirculation loops.

For the gas turbine part, exergy losses for the independent components, namely the combustion chamber, the turbine and the air compressors and the water pump are added together for calculating the total loss. In a similar manner, the losses in the heat exchangers used to recover heat from the gas turbine exhaust and the heat exchangers used to recover waste heat from the gas-cleaning loop are added together to calculate the losses in the heat recovery part.

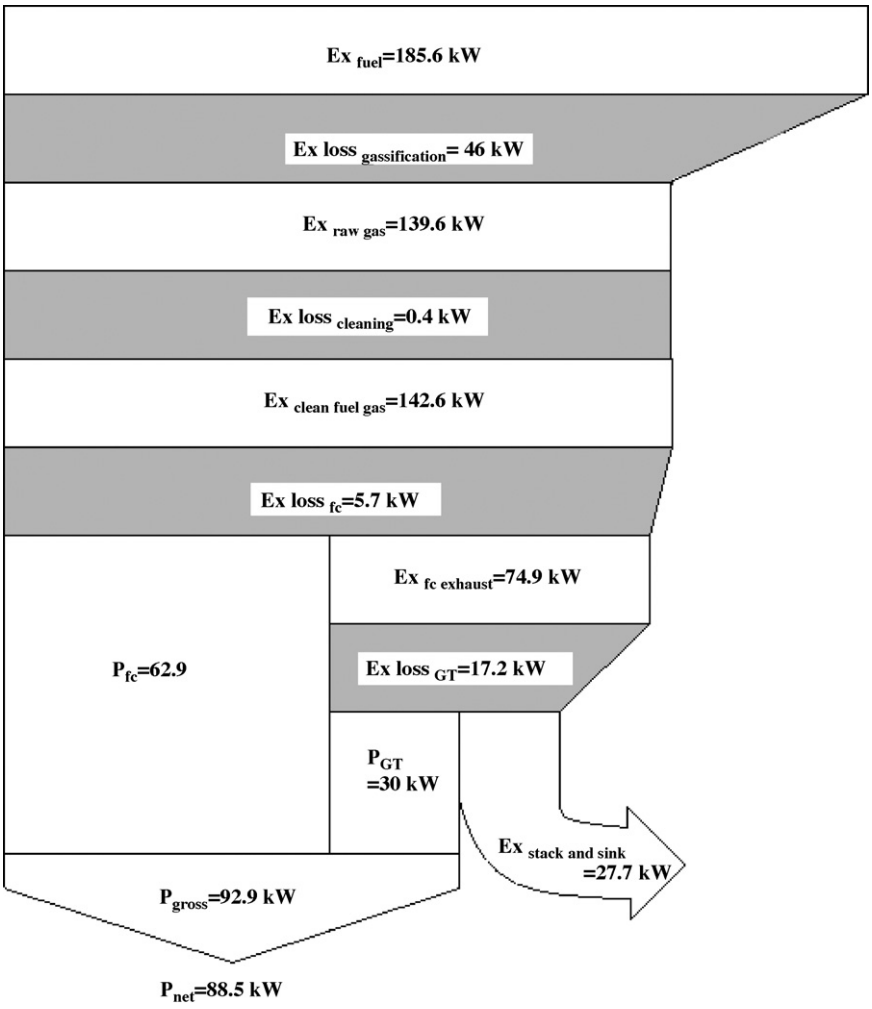

Fig. 6. Simplified Grassmann diagram indicating the exergy flows in the base case system.

Gas turbine exhaust after the heat recovery has temperatures higher than the defined stack temperature of 373 K. A heat sink is employed to calculate the available energy and exergy in the stream when cooling the exhaust flow to stack temperature. Energy and exergy available at the stack are considered to be the losses to the environment. It is assumed that the exergy available at the heat sink can be made use of by employing an appropriate conversion method and is not considered as a loss here.

5. Gas cleaning at different temperatures and the impact of steam addition

5.1. Gas cleaning at lower temperatures

Though a system with lowest gas-cleaning temperature at 873 K is presented initially, techno economical conditions prevailing in different situations may cause to consider various other gas-cleaning options with different lowest cleaning temperatures. The facts that the tolerance levels of SOFCs to various contaminants are not well defined and the high-temperature gas-cleaning systems are still under various stages of development also bring in uncertainties in selection of proper gas-cleaning systems. Different lowest cleaning temperatures in turn will require different levels of steam addition to suppress carbon deposition at those temperatures. It is also possible that heat exchangers employed in the system may have cold spots with temperatures lower than the lowest gas-cleaning temperature. Such conditions will also cause carbon deposition and additional steam may have to be used to prevent it. This section presents the analysis on influence of different lowest temperatures in the gas-cleaning units and hence the steam addition required on the system performance.

In this section, an analysis of system performance with different gas-cleaning temperatures is presented. Systems are considered with up to 30% steam addition, which corresponds to a lowest gas-cleaning temperature of 555 K. Only dry gas-cleaning processes are considered. Atmospheric temperature gas cleaning is not treated here and will be presented later in this paper separately. Values assigned to various system parameters, other than the gas-cleaning unit components, remain same.

If a reliable cleaning system can be designed with lowest cleaning temperatures around 1023 K, there will be no need of steam addition. Since high-temperature gas-cleaning processes with different lowest gas-cleaning temperatures are currently being developed, and techno economical viability of these systems will depend upon the results of these development activities, it is not attempted here to provide details of such gas-cleaning concepts. However, for giving an indication, examples of various possible gas-cleaning options, which may cause such temperature limitations, are given briefly. Though such systems are not necessarily available at present, it is interesting to explore the thermodynamic consequences of opting for such systems. Possible variations in pressure drops across gas-cleaning reactors are ignored for this simplified analysis.

Various possible options for gas cleaning with different lowest temperatures are briefly mentioned as the following.

(1) Lowest gas-cleaning temperature between 1023 K and 823 K. If HCl cleaning is altogether avoided and if few tens of ppms of H_2S in biosyngas is no problem for SOFCs, zinc titanate could be used for sulfur cleaning at higher temperatures. (Tolerance of SOFCs for HCl and H_2S is discussed elsewhere [1,3], and if the initial results can be confirmed with long-term experiments, such possibilities of high tolerance levels may emerge in future). Tar and particulate cleaning is suggested at gasification temperature. An alkali getter can be suggested at SOFC inlet temperature.
(2) Lowest gas-cleaning temperature 823 K to 673 K: Lower temperatures till 673 K may represent systems with ZnO employed for H_2S cleaning at various temperatures. At these temperatures sodium carbonate can be used for HCl cleaning at the same temperatures as that of ZnO sorbent. Tar and particulate cleaning is suggested at gasification temperature. An alkali getter can be suggested at SOFC inlet temperature. Alternately particles can also be removed close to H_2S and HCl cleaning temperatures and this will help to remove a part of the alkalis as well.
(3) Still lower temperatures and hence higher steam addition values such as 25% and 30% may represent cases in which low-temperature filters such as bag filters are employed for particulate cleaning after a tar reformer working at near gasifier temperature. (With other gas-cleaning devices HCl and H_2S cleaning either working at lower temperatures or altogether are avoided). Alkalis are expected to be removed at low-temperature particle filter.

As the temperature of the gas is brought down for low-temperature cleaning, the tendency for carbon deposition increases. To avoid this, steam addition is required. Carbon deposition tendency with varying steam addition is studied using chemical equilibrium computations. Fig. 7a shows the variation in carbon deposition temperature with steam addition. The gas compositions with varying steam addition used in the chemical equilibrium computations are taken from the results of system calculations with varying steam addition. Once the gas composition is known, the temperature at which the carbon deposition tendency begins for that particular gas composition is found using chemical equilibrium calculations carried out using the software Factsage. Once this temperature is known, the lowest temperature in the gas-cleaning system is set at 10 K above the temperature at which the carbon deposition tendency begins.

Mass flows through the system and hence the power level is set by the turbine power fixed at 30 kW. As more steam is added, and there is no significant variation in the turbine inlet temperature and since the pressure ratio is fixed, the mass flow through the turbine decreases. This causes lower fuel and air input to the system and hence the total energy input to the system decreases. As the fuel flow comes down and as the steam content in the fuel is increased, the power produced from the fuel cell also comes down. These variations are shown in Fig. 7b. System calculations with steam addition to the gas have indicated two general trends. Added steam is causing a decrease in the SOFC efficiency and improves the performance of the gas turbine (% conversion in the gas turbine is calculated approximately by dividing the gas turbine power output by the difference between total input energy and the electricity produced from the fuel cell). In the fuel cell this is in line with expectations as the Nernst voltage is affected when the steam fraction is increased in the gas. The increase in the performance of the gas turbine cycle within certain range of steam addition is reported before [19]. However, there are no significant changes in the total electrical efficiency of the system and it is observed that the system efficiency stays around 54% with a steam addition increase from 0% to 30%. Changes in the performance of the fuel cell and gas turbine as well as the variation in total efficiencies are described in Fig. 7c and d.

Even though the electrical efficiency stays same with steam addition, it is observed that the available heat energy that can be extracted from the system outlet stream before it goes to the stack at 373 K decreases. This happens due to the following reason. In the case of no steam addition, even though the gas turbine outlet stream is used to preheat the cathode air and gasification air, still the flue gas temperature remains high at 621 K. In systems with no steam addition, this energy is still available to be harnessed with bottoming cycles or with heat extraction for suitable applications. But as the steam addition is increased, this consumes heat energy from

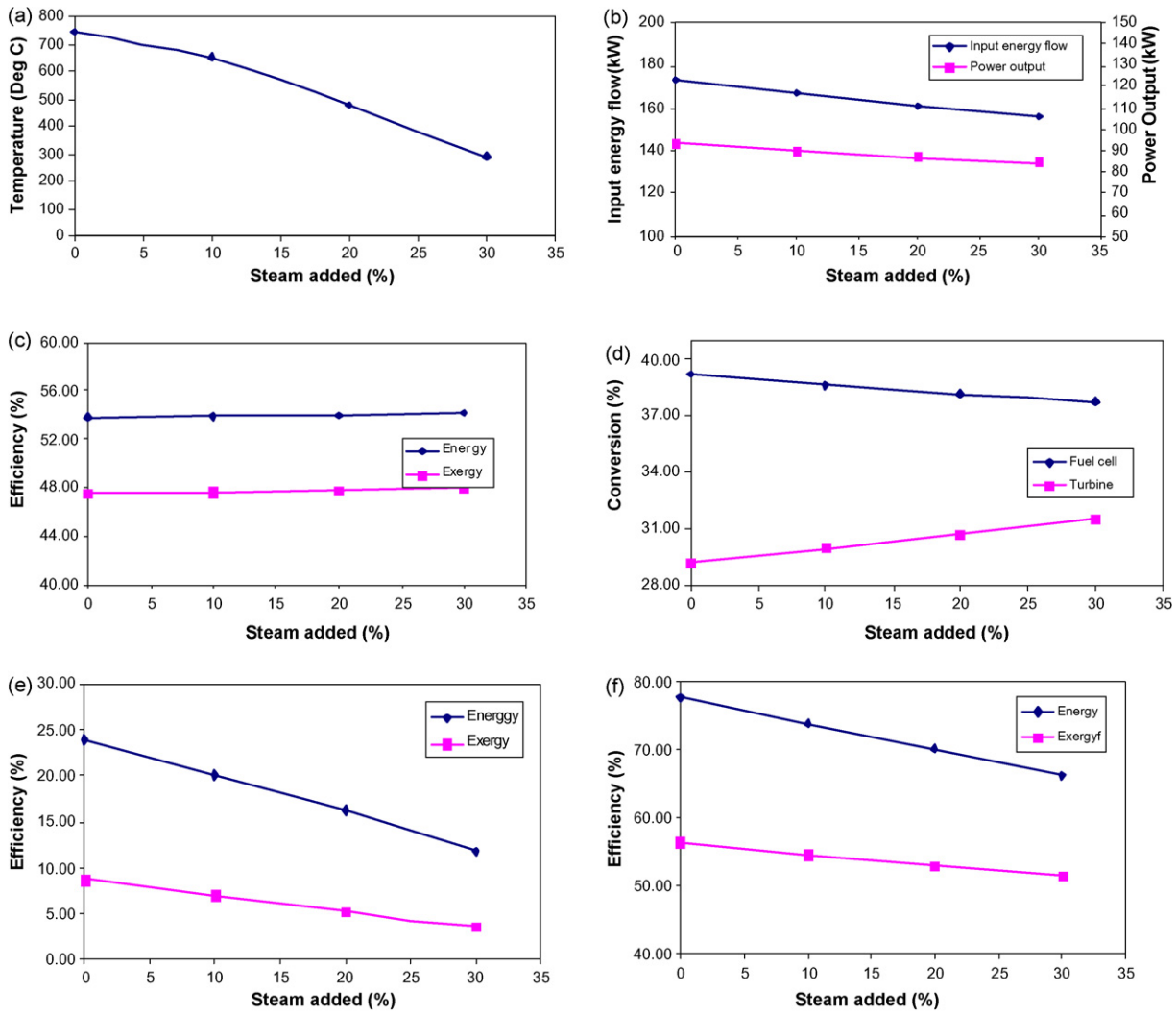

Fig. 7. (a) (left) Variation in carbon deposition temperature with varying steam addition. (b) (right) Input energy flow and power delivered with varying steam addition. (c) (left) Energy (electrical) and exergy efficiency of the presented system with varying steam addition. (d) (right) Variation of the fraction of input energy converted in fuel cell and gas turbine with steam addition. (e) (left) Thermal energy and exergy efficiency as a percentage of the fuel input with varying steam addition. (f) (right) Total energy and exergy efficiency in case of varying steam addition.

the gas turbine outlet stream to get superheated and the outlet gas temperature before it enters the stack decreases. With 30% steam addition, this temperature is brought down from 621 K (at 0% steam) to 496 K. The heat available from the sink is reduced from 41.3 kW without steam addition to 18.5 kW at 30% steam addition. This reduces the total efficiency even while keeping the system electrical efficiency at comparable levels. Exergy value of this stream is low as its temperature is low. Thermal energy and exergy efficiencies are presented in Fig. 7e as a function of steam addition. Total energy and exergy efficiencies with varying steam addition are given in Fig. 7f.

With the addition of steam, as more water is added to supply the steam, and most of the steam passes through the stack to the outlet, the system energy efficiency comes down. It can be seen that (Fig. 8) the stack latent heat loss increases with increased steam addition. In fact, this is the major reason for lower system thermal efficiencies at increased steam addition. The other two major losses, namely the stack losses and the gasifier losses (mainly due to carbon separation) do not vary much.

Fig. 9 gives the split up of exergy losses in the system with varying steam addition. It can be seen that the exergy loss due to the heat loss to the environment increases, as the steam content is higher. As the heat transferred in the heat recovery process increases with steam addition, associated exergy losses are also expected to increase. It can be seen that variation in the exergy losses in fuel cell as well as gas turbine are rather insignificant thereby keeping the variations in the net electrical efficiencies insignificant.

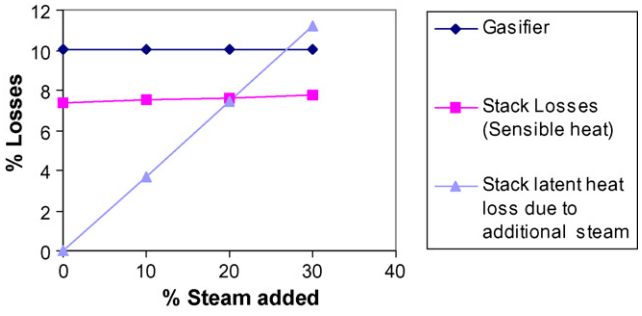

Fig. 8. Energy losses with varying steam addition.

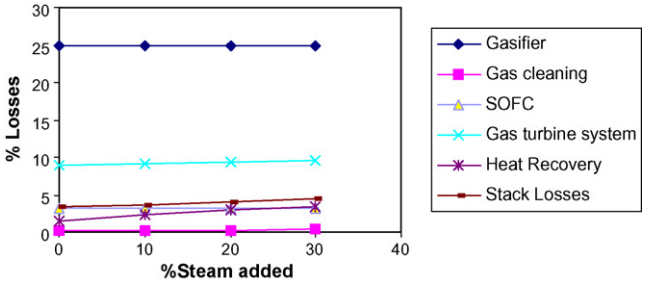

Fig. 9. Exergy losses with varying steam addition.

6. Gas cleaning at atmospheric temperature

In this section, thermodynamic implications of opting for atmospheric temperature gas cleaning are presented. These results are then compared with the results from calculations performed for systems with high-temperature gas cleaning. The gas-cleaning system considered comprises the following. Cleaning with wet scrubbers can bring down the gas temperature rapidly and it is assumed that carbon deposition is not favored in such conditions. Even if solid carbon is formed, it often gets removed with the scrubbing liquid. HCl, H_2S and alkalis are also expected to get removed with scrubbing. Steam in the gas is also condensed out during scrubbing. A barrier filter shall then be used for particulate cleaning. Unlike during scrubbing with liquid where sudden cooling may not favor carbon deposition (and even if the carbon is formed, it will probably get removed with scrubbing liquid), slow heating up in heat exchangers may still cause carbon deposition. For this reason, additional steam is added after the gas is cooled and cleaned to suppress carbon deposition while the gas is heated on its way to the fuel cell inlet. A split stream from the gas turbine exhaust is employed to heat up the clean gas to 673 K and this gas is then mixed with a part of the anode outlet stream to heat the gas before it is fed to the anode (Fig. 10). When compared to the models with high-temperature gas cleaning, the added water for steam production is heated using only one heat exchanger since in any case the mixture of fuel gas and the extra steam is heated to 673 K in a different heat exchanger. Rest of the system configuration stays same as in the case of proposed high-temperature gas-cleaning system.

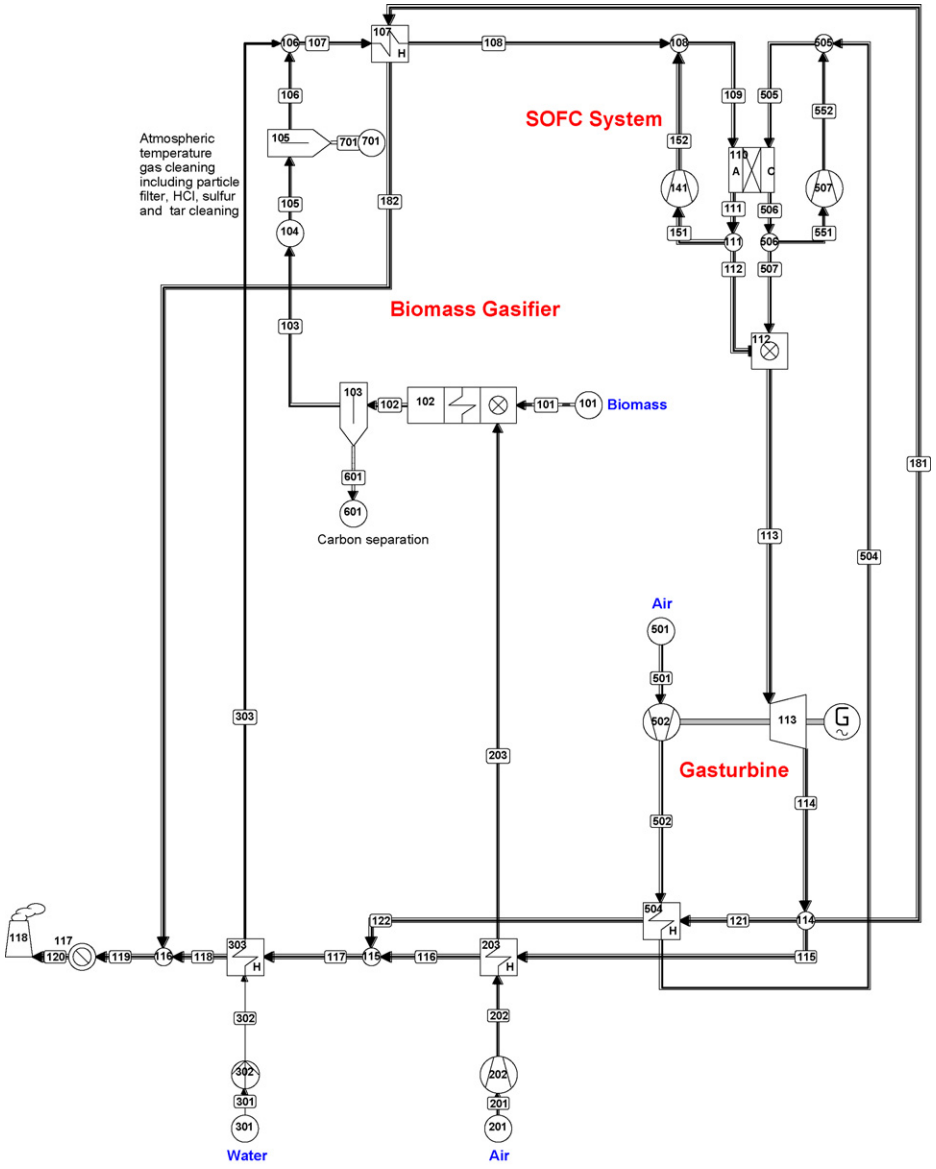

Fig. 10. Flow diagram for the system with gas cleaning at atmospheric temperature.

Table 6
System efficiency with extra steam addition to prevent carbon deposition with case 1.

	Apparatus	Energy flow [kW]	Totals [kW]	Exergy flow [kW]	Totals [kW]
Absorbed power	Sink/source	199.16	199.16	225.48	225.48
Delivered gross power	Generator	30.00	104.36	30.00	104.36
	Fuel cell	74.36		74.36	
Auxiliary power consumption			5.49		5.49
Delivered net power			98.87		98.87
Delivered heat	Heat sink		14.56		4.72
Total delivered			113.43		103.59
Efficiencies					
Gross		52.40%		46.29%	
Net		49.64%		43.85%	
Heat		7.31%		2.09%	
Total		56.96%		45.94%	

The influence of parameters like residence time of the gas flow within the considered region, catalytic activity of the surface with which the gas is in contact, etc., may have a significant influence on carbon deposition in addition to thermodynamics. Practical implications of this could be that a gas composition with thermodynamic possibility of carbon deposition at given conditions may not cause deposition when it passes through a gas pipe with a short residence time and might cause deposition when it is exposed to a catalytically active surface of the gas-cleaning reactors with a high gas residence time. Observation of carbon deposition from biosyngas while it is heated from ambient temperature to the SOFC inlet temperature of 1123 K was reported elsewhere [1]. When enough steam was added to suppress carbon deposition above 873 K, formation of solid carbon disappeared even at lower temperatures. Based on our observations in the laboratory as reported before and the information from literature, it can be considered that this amount of steam can be sufficient to prevent carbon deposition when, (1) the gas is being heated or cooled during its passage through the gas pipes with sufficient gas velocity, (2) the pipe surface is not catalyzing carbon deposition reactions at these temperatures, and (3) there is no other system component in between, such as gas-cleaning devices, which may require high residence time for the gas (It has been reported that, in practice, for preventing carbon deposition from synthesis gas containing carbon monoxide, usually less steam than what is thermodynamically required is sufficient [20]). However, our experience is not sufficient to confirm that, with this level of steam addition, in all conditions carbon deposition will be prevented while being heated when the gas residence times or gas carrying pipe surfaces are totally different. This introduces the possibility that higher amount of steam is required for preventing carbon deposition in certain cases. For this reason, two sets of calculations are presented here assuming two different scenarios.

Case 1 (Low steam addition): It is assumed that there will be no carbon deposition when sufficient steam is added to suppress the deposition tendency at 873 K. Results are given in Table 6. When 19.4% additional steam is added to avoid carbon deposition at 873 K, the electrical efficiency was observed at 49.6% and total efficiency was observed at 57%.

Case 2 (High steam addition): All the waste heat available with the system is used for steam generation and this steam is added to the syngas before it is heated up. Results are given in Table 7. It is seen that with the present system configuration, the upper limit of possible steam generation is 32% (by mass%) of the biosyngas. It is also observed that the gas composition is thermodynamically safe with this amount of steam at 503 K and above. When 32% extra steam was added, electrical and total efficiency values were observed to be lower at 49.5% and 49.9% respectively. It can be observed that addition of steam does affect the total efficiency much more than the electrical efficiency. This can be attributed to the fact that steam generation is done using the heat that cannot be transferred to the cathode air or gasification air. And this increased steam production reduces the heat that can be delivered from the system.

Results so far indicate the following. With low-temperature gas cleaning, it is possible to get high electrical efficiencies of

Table 7
System efficiency with extra steam addition to prevent carbon deposition with case 2.

	Apparatus	Energy flow [kW]	Totals [kW]	Exergy flow [kW]	Totals [kW]
Absorbed power	Sink/source	190.38	190.38	215.55	215.55
Delivered gross power	Generator	30.00	99.50	30.00	99.50
	Fuel cell	69.50		69.50	
Auxiliary power consumption			5.28		5.28
Delivered net power			94.22		94.22
Delivered heat	Heat sink		0.76		0.18
Total delivered			94.99		94.40
Efficiencies					
Gross		52.27%		46.16%	
Net		49.49%		43.71%	
Heat		0.40%		0.08%	
Total		49.89%		43.80%	

the order of 50% even for small-scale power plants of the order of 100 kW. If there is a specific heat consumer available (for the low-temperature waste heat), it might be possible to design power plants with a total efficiency of 57% by minimizing the steam added for preventing carbon deposition. However, if there is no specific heat consumer available, plants with high steam addition (case 2) may offer wider choices for plant design in terms of the acceptable gas flow velocities and materials of power plant construction (without sacrificing the electrical efficiency significantly).

6.1. Comparison between high-temperature gas cleaning and low-temperature gas cleaning

For systems with biomass gasifiers (with air as gasification agent), solid oxide fuel cells and gas turbines, it is possible to achieve electrical efficiencies of the order of 54% and total efficiencies of the order of 77–78%, if gas cleaning is possible at high temperatures around 1023 K. As the gas-cleaning temperature comes down, steam addition will be required to suppress carbon deposition and this steam can be generated using heat from the turbine exhaust. With steam added, electrical efficiency stays around 54% but the total efficiency decreases significantly. With a steam addition of 30%, the total efficiency comes down to 66%.

Cleaning at ambient temperatures with wet scrubbers employed as considered here causes the loss of sensible heat of the gas. This brings down the system efficiency values. With two cases of low-temperature gas cleaning presented here, electrical efficiency appeared to be 49.6 with low steam addition case (case 1) and 49.5 with high steam addition case (case 2). Total efficiency obtained is 57% and 49.9%, respectively (Tables 6 and 7).

It is shown that gasifier–SOFC–gas turbine systems with ambient temperature gas cleaning are also capable of providing electrical efficiencies close to 50% (~4–5% less when compared to high-temperature gas-cleaning systems). However the total efficiency is significantly lower for systems with ambient temperature gas cleaning when compared to high-temperature gas cleaning.

The discussion presented above clearly indicates that the gas-cleaning systems have to be chosen carefully according to the conditions at the places where such plants are built. In general electrical efficiency should be given importance. If there are opportunities for utilizing the waste heat, then there are certain advantages with high-temperature cleaning systems. However, if there are no suitable means for using the waste heat and/or if the low-temperature gas cleaning is offering a cheap and easy option when compared to hot gas cleaning, such systems can be employed still with very high electrical efficiencies when compared to competing systems such as gasifier-reciprocating engines with electrical efficiencies around 15–25% [21].

7. Conclusions

The system calculations performed indicate that high system electrical efficiencies around 54% are achievable in small-scale gasifier–SOFC–GT systems of the order of one hundred kW or more. It is possible to achieve these efficiencies with a wide range of gas turbine pressure ratios (variation in pressure ratios between 4.5 and 7 did not show any significant effect on system efficiency). In general, if the gas cleaning employed in such systems are at lower temperatures when compared to the gasification temperature of 1073 K, additional steam will have to be added to have conditions thermodynamically unfavorable for carbon deposition (In the system considered in the present study, cooling the gas below 1023 K starts carbon deposition tendencies). Gas cleaning at lower temperatures and steam addition thus required did not have significant impact on system electrical efficiency, which stayed around 54%. However, generation of additional steam using heat from gas turbine outlet will decrease the thermal energy and exergy available at the system outlet thereby decreasing the total system efficiency. Addition of 30% steam (by mass percentage of the biosyngas) decreased the total efficiency from 78% to 66% while variation in total exergy efficiency is relatively smaller with a decrease from 56.3% to51.4%. It can be noted that, in general, obtaining higher electrical and exergy efficiencies is of greater importance.

It is possible to get electrical efficiencies near 78% with small-scale SOFC–GT systems running with methane [1]. But when the same SOFC–GT system is adopted for biomass gasifier–SOFC–GT systems, the total system efficiency comes down drastically. Gasification losses, including solid carbon lost during gasification constitutes a major reason for energy and exergy losses. If the quantity of this carbon is reduced or if this carbon can be used back in the system, the system efficiency will increase by few percentages. Another possibility is to use the carbon separated as raw material for processes such as activated carbon generation. Endothermic methane reforming in SOFC is another possible reason for high efficiencies for systems running on methane steam mixtures.

It is also seen that preheating of gasification air is increasing the electrical efficiency of the system while the total efficiency slightly decreases (as shown in Appendix B). When preheating of the gasification air is avoided, it is observed that the system electrical efficiency came down to 50.7% from 53.94% and the net efficiency has slightly increased to 73.6% from 72.3%. However, total exergy efficiency decreased from 53.8% to 53.1%.

With gas cleaning at atmospheric temperature, there is a decrease in the electrical efficiency of the order of 4–5% when compared to the base case system with high-temperature gas cleaning. Small-scale biomass gasifier–SOFC–gas turbine systems, even with low-temperature gas cleaning, offer significantly higher efficiencies when compared to competing technologies such as gasifier-reciprocating engine systems. However, with the fact that low-temperature gas-cleaning systems are much more technologically matured, it can be concluded that low-temperature gas cleaning is attractive, but high-temperature gas cleaning enables further increase of the system efficiency.

In general, this analysis indicates that for small-scale systems of few hundred kW, gasifier–SOFC–GT systems have significant advantages in terms of improved efficiency over other systems of comparable scales like gasifier-reciprocating engine systems and their development needed to be pursued seriously.

Acknowledgement

First author, PV Aravind wishes to acknowledge the help and support received from Prof. J. Schoonman during the work presented in this paper.

Appendix A. System with gas cleaning at gasifier outlet temperature

This appendix provides a concept for a much simplified gas-cleaning system based on the studies on the influence of biomass derived contaminants. For the SOFCs with Ni/GDC anodes and gas turbines, it is assumed that few tens of ppms of H_2S and HCl as present in biosyngas may not cause any significant problem [1,3,5,10]. Then particulates are removed using a high-temperature filter, and tars are removed using a dolomite and nickel-based tar reformer and alkalis are removed using an alkali getter (Fig. A.1). There is no lowering of the temperature for gas cleaning and the gas from the gasifier, after cleaning at 1073 K is fed to the SOFC anode through a final particulate filter. As a few ppms of H_2S is expected in the fuel gas, an additional internal sulfur tolerant

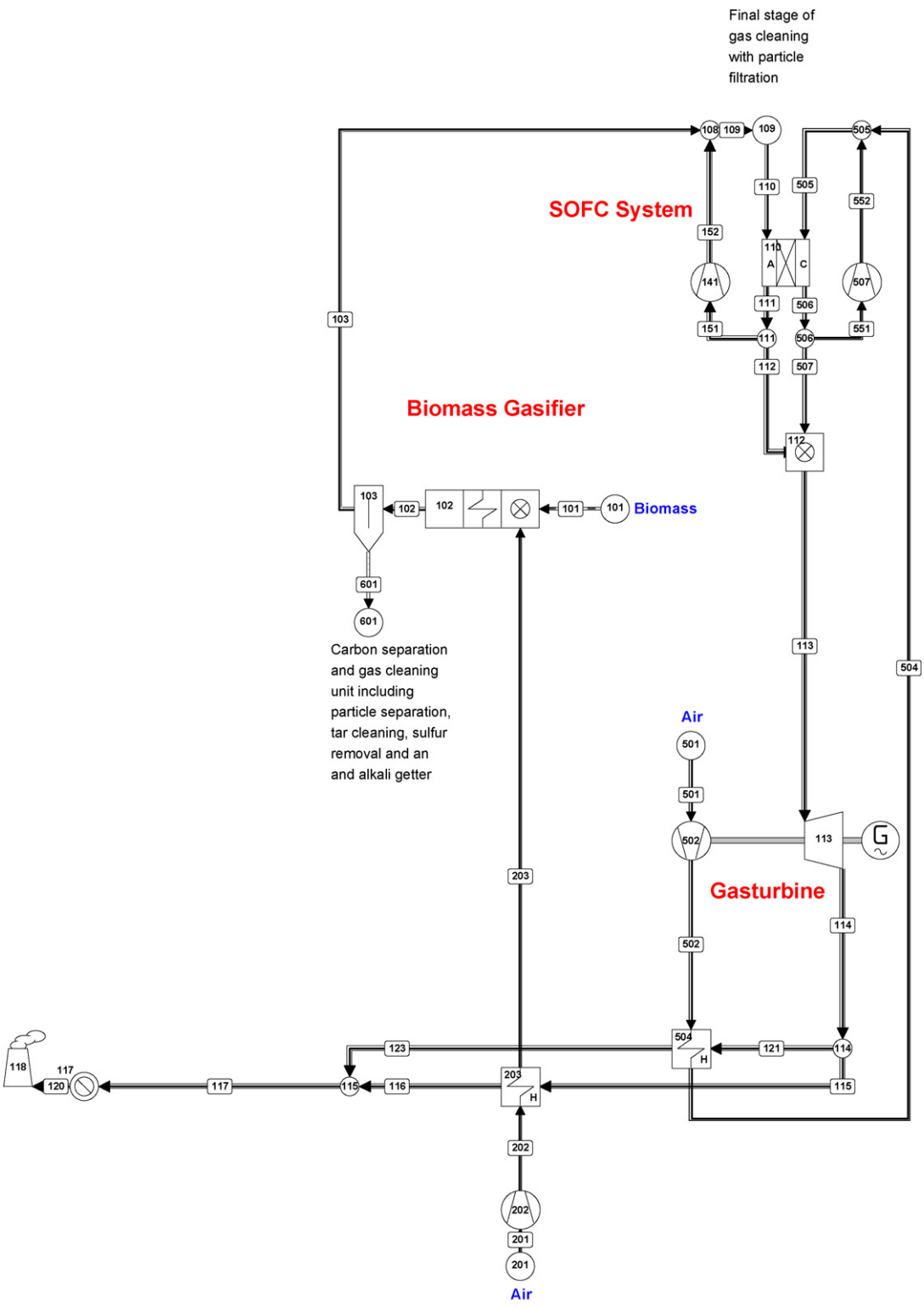

Fig. A.1. Flow scheme for the system with gas cleaning at gasifier outlet temperature.

methane reformer with direct heat exchange with the stack, operating at stack temperature is proposed. Rest of the system remains same and the results from the system calculations are given in Table A.1. It is observed that the system electrical efficiency is slightly higher at 54.2% when compared to gas cleaning at lower temperatures. Same is the case with total efficiency which stays at 77.8%.

Appendix B. Comparison of systems with and without preheating of gasification air

To understand the effect of preheating the gasification air, a set of calculations is carried out with the gasification air fed to the gasifier directly after compression without any preheating. As in the standard case, the gas-cleaning temperature is kept at 873 K. How-

Table A.1
Various efficiency values for the power plant based on gas cleaning at gasifier outlet temperature.

	Apparatus	Energy flow [kW]	Totals [kW]	Exergy flow [kW]	Totals [kW]
Absorbed power	Sink/source	171.04	171.04	193.55	193.55
Delivered gross power	Generator	30.00	97.32	30.00	97.32
	Fuel cell	67.32		67.32	
Auxiliary power consumption			4.59		4.59
Delivered net power			92.73		92.73
Delivered heat	Heat sink	40.33	40.33	16.52	16.52
Total delivered			133.06		109.25
Efficiencies					
Gross		56.90%		50.28%	
Net		54.21%		47.91%	
Heat		23.58%		8.54%	
Total		77.79%		56.44%	

Table B.1
Efficiency values obtained from system calculations with no gasification air preheating.

	Apparatus	Energy flow [kW]	Totals [kW]	Exergy flow [kW]	Totals [kW]
Absorbed power	Sink/source	169.69	169.69	192.12	192.12
Delivered gross power	Generator	30.00	91.20	30.00	91.20
	Fuel cell	61.20		61.20	
Auxiliary power consumption			5.13		5.13
Delivered net power			86.07		86.07
Delivered heat	Heat sink	38.87	38.87	15.99	15.99
Total delivered			124.94		102.07
Efficiencies					
Gross		53.74%		47.47%	
Net		50.72%		44.80%	
Heat		22.91%		8.33%	
Total		73.63%		53.13%	

ever, the steam required to be added to have no carbon deposition came down from 14.4% to 11.4%. As the air is fed to the gasifier at atmospheric temperature, more air is consumed when compared to the gasification with preheated air. This increases the percentage oxygen in the product gas and hence less steam is required to take it to safe region for avoiding carbon deposition. Table B.1 gives the efficiency values obtained from the calculations. When preheating of the gasification air is avoided, it is observed that the system electrical efficiency came down to 50.7% from 53.94% and the net efficiency has slightly increased to 73.6% from 72.3%. However, total exergy efficiency decreased from 53.8% to 53.1%. As it was in the case of base case system, it is observed that the process with highest exergy destruction is gasification. When preheating of gasification air is avoided, the percentage exergy loss during gasification increased from 24.9% to 26.3%. This can mainly be attributed to the increase in air intake which increases the exergy loss.

References

[1] P.V. Aravind, Studies on high efficiency energy systems based on biomass gasifiers and solid oxide fuel cells with Ni/GDC anodes, PhD Thesis, 2007, TU Delft.
[2] P.V. Aravind, J.P. Ouweltjes, E. de Heer, N. Woudstra, G. Rietveld, Electrochemical Society Proceedings 7 (2005) 1459–1467.
[3] P.V. Aravind, J.P. Ouweltjes, N. Woudstra, G. Rietveld, Electrochemical and Solid-State Letters 11 (2008) B24–B28.
[4] S. Baron, N. Brandon, A. Atkinson, B. Steele, R. Rudkin, Journal of Power Sources 126 (2004) 58–66.
[5] J.P. Ouweltjes, P.V. Aravind, N. Woudstra, G. Rietveld, Journal of Fuel Cell Science and Technology 3 (2006) 495–498.
[6] K.D. Panopoulos, L.E. Fryda, J. Karl, S. Poulou, E. Kakaras, Journal of Power Sources 159 (1) (2006) 570–585.
[7] C. Athanasiou, F. Coutelieris, E. Vakouftsi, V. Skoulou, E. Antonakou, G. Marnellos, A. Zabaniotou, International Journal of Hydrogen Energy 32 (3) (2007) 337–342.
[8] A.O. Omosun, A. Bauen, N.P. Brandon, C.S. Adjiman, D. Hart, Journal of Power Sources 131 (1–2) (2004) 96–106.
[9] P.V. Aravind, MSc Thesis. 2001, University of Oldenburg.
[10] D. Thimsen, Assessment of Fuel Gas Cleanup Systems for Waste Gas Fueled Power Generation, Electric Power Research Institute Palo Alto, CA, 2006.
[11] www.cycle-tempo.nl.
[12] H.S. Mukunda, P. Paul, S. Dasappa, U. Shrinivasa, N.K.S. Rajan, H. Sharan, R. Beuhler, P. Hasler, H. Kaufmann, Energy for Sustainable Development 1 (1994) 46–49.
[13] Phyllis, database for biomass and waste, http://www.ecn.nl/phyllis. Energy research Center of the Netherlands.
[14] www.factsage.com
[15] K.J. Bosch, N. Woudstra, K.V. van der Nat, Proceedings of the 4th International Conference on Fuel Cell Science, Engineering and Technology, Irvine, CA, 2006.
[16] B.J.P. Burhe, MSc Thesis. 2000. Technical University Delft.
[17] H. Cohen, G. Rogers, H. Saravanamuttoo, Gas Turbine Theory, Addison Wesley Longman Limited, 1996.
[18] M.J. Prins, K.J. Ptasinski, Energy 30 (2005) 982–1002.
[19] Y.C. Huang, C.I. Hung, Z. Cheng, Journal Proceedings of the Institution of Mechanical Engineers. Part A. Journal of Power and Energy 214 (2000) 61–73.
[20] E. Deurwaarder, H. Boerrigter, H. Mozaffarian, L.P.L.M. Rabou, A. van der Drift, Proceedinngs of the 14th European. Biomass Conference & Exhibition, Paris, France, October 17–21, 2005, 2005.
[21] G. Sridhar, P.J. Paul, H.S. Mukunda, Biomass and Bioenergy 21 (1) (2001) 61–72.